Hindawi
Journal of Nanomaterials
Volume 2022, Article ID 2928601, 14 pages
https://doi.org/10.1155/2022/2928601

Research Article

Influence of New Energy Materials on Dynamic Interaction between Surrounding Rock and Structure of Heavy-Duty Railway in Small Clearance Crossing Tunnel

Xiaotian Hao[1,2] **and Hailong Wang**[1,3]

[1]*School of Traffic and Transportation, Shijiazhuang Tiedao University, Shijiazhuang, 050043 Hebei, China*
[2]*School of Urban Construction Engineering, Chongqing Technology and Business Institute, Chongqing 400052, China*
[3]*School of Civil Engineering, Hebei University of Architecture, Zhangjiakou, 075000 Hebei, China*

Correspondence should be addressed to Hailong Wang; bhxt196346@cqtbi.edu.cn

Received 3 March 2022; Revised 28 June 2022; Accepted 7 July 2022; Published 11 August 2022

Academic Editor: Awais Ahmed

Copyright © 2022 Xiaotian Hao and Hailong Wang. This is an open access article distributed under the Creative Commons Attribution License, which permits unrestricted use, distribution, and reproduction in any medium, provided the original work is properly cited.

In the rapid development of urban traffic, the small clearance interchange tunnel has always been a difficult problem for heavy-duty railways, so special requirements are also put forward for materials. Bainite steel with excellent comprehensive mechanical properties is considered to replace traditional high manganese, the best material for steel. This article first improves the process of the material and analyzes the structural dynamics of the material through different isothermal cooling to analyze the different performances of the material on the heavy-duty railway. Using traditional theoretical data analysis, theoretical data calculation, numerical analysis simulation, and on-site engineering monitoring technical means is to complement the construction of the soft rock underground tunnel in the subway section at the intersection of the small clear distance line to the existing surrounding rock tunnel wall in the section. The degree of deformation affects the change law, and the related technical issues of engineering control are analyzed. Finally, the control measures of full-face grouting reinforcement with steel flower pipes and the final construction plan of constructing the left line, right line, and undercut section in sequence are proposed. FLAC numerical simulation software was used to complete the feasibility evaluation of the control measures for the deformation of the ground and lining induced by the construction of the cross tunnel. The results show that the maximum deformation of the ground surface is reduced by 35.4% compared with no control measures, and the longitudinal deformation range of the ground surface and the vault is reduced by 28.9%.

1. Introduction

Throughout the world of underground cities, the smooth utilization, development, and comprehensive utilization of public space in underground cities have been rapidly developed and gradually become an effective and important way to effectively solve the serious crisis of underground resources and local soil ecological environment pollution in various underground cities. After our country has entered the 21st century, our country's underground and aboveground urban rail transportation vehicle transportation system infrastructure has initially entered a new stage of rapid, healthy, and orderly development. According to statistics, as of the end of 2016, a total of 30 major large- and medium-sized cities in northern mainland China have completed and opened underground and aboveground urban rail transit automobile public transportation, a total of 133 operating subway lines, and a total of annual operating subway line mileage. The maximum length is 4152.8 kilometers, of which the cumulative operating mileage of Beijing Metro in 2016 was 3168.7 kilometers, accounting for 76.3%. Construction of Nanning Metro began in 2011, and Line 1 was opened

for operation in September 2016. Up to now, Nanning has planned 8 lines, including 187 stations, 22 transfer stations, and 4 vehicle lines.

With the continuous increase in the depth of underground space excavation and planned mileage, the number of stations and transfer stations will also continue to increase, and the cross construction of two or more tunnels will become increasingly apparent. In addition, due to the dense high-rise buildings in the urban areas of our country and the developed subway underground tunnel transportation network, the building pile foundations, municipal tunnel pipelines, underground tunnel structures, and other ancient buildings during the construction of subway underground tunnels have formed the use of space in the urban newly built subway tunnels. Large space restrictions cannot be avoided by design. Therefore, the probability of overlap between new tunnels and existing tunnels is greatly increased. However, the continuous construction of the existing new building tunnels will cause great disturbance to the surrounding building stratum structure, causing three or even four times of large stress between the existing new tunnel and the structural stratum, causing the existing new tunnel and steel structure stratum to occur the stress adds a large internal force and stratum deformation, causing sudden surface deformation values, and there is a major construction risk. Excessive deformation of the tunnel may directly cause the main structure of the existing domestic road tunnels to fail to fully meet the road operation safety requirements, and the ground will also have depressions. When severely damaged, road operations and traffic safety accidents will occur directly and cause great operational safety hazards. In order to ensure the safe and smooth operation of our country's urban rail network transportation, how to effectively supervise, control, and accurately evaluate the direct impact of the delayed construction of urban new railway tunnels on the existing urban new tunnels has gradually become a key academic research topic today.

At present, the research on the influence of new energy materials on the dynamic interaction between the surrounding rock and structure of the heavy-duty railway tunnel with a small clear interval is mainly in these directions. Yanowitz et al. layered the dolomite and rock limestone together and performed a separate downgrading modulus treatment. There was a problem that the dolomite rock surrounding rock model hierarchical modulus was low. According to the surrounding rock model ED (China Dynamics Yang) for tunnel engineering along the Chengdu-Chongqing Railway Modulus classification and quantitative model classification processing system, the dolomite surrounding rock is separately downgraded, which solves the problem of low dolomite surrounding rock model classification modulus, but the materials targeted in this direction are relatively limited [1]. Correa et al. established a three-dimensional numerical prototype virtual statistical model of the length of the subway tunnel based on the various geological surrounding rock deformation risk conditions in the domestic subway tunnel site engineering design and the results of this research, and calculated the collapse of the base layer of the domestic subway exit tunnel through the tunnel numerical prototype simulation, the design process of the surrounding rock deformation during the construction, and the analysis of the deformation process of the base layer of the subway tunnel. After the design is completed, the exit tunnel of the existing domestic subway tunnel station exit tunnel and the newly built foreign existing domestic expressway Yangtze River Bridge station tunnel subway base collapsed surrounding rock statistics on the relatively large risk of construction deformation due to the collapse of the arch bottom. It is concluded that there may be a high-strength plasticity metro tunnel arch underneath part of the area under the subway arch of the newly built domestic existing expressway station tunnel, and there may be a greater risk of deformation of the surrounding rock when the base of the subway tunnel collapses. There is a certain amount of simulated data [2]. In the actual construction design stage of the railway elevated tunnel project, Yamada et al. formulated practical and feasible overall construction technology according to the actual construction situation of the weak layer and the horizontal hard rock layer in the railway tunnel, in order to effectively ensure the entire tunnel construction design project. Quality and safety are effectively guaranteed, and a detailed discussion of how the overall construction technology of the horizontal hard rock layer of the tunnel should be applied in the actual railway tunnel engineering construction design process is given, but the research is too theoretical [3]. Liu et al. conducted a comprehensive analysis of the movement measurement of the local stress and deformation of the surrounding rock structure of 8 underground tunnels located in 12 shallow and deep buried sections of the underground tunnel, and analyzed the tunnel surroundings of each section of the shallow tunnel under the shallow and deep buried section of the underground tunnel. The research and analysis results of the local movement and deformation of the rock structure's overall movement law are compared and analyzed in depth. The research and analysis of the overall local deformation movement law of the surrounding rock structure of each section of the underground tunnel is divided into the first rapid movement displacement of the surrounding rock of the underground tunnel-rapid movement displacement stable deformation—slow motion displacement stabilizes deformation—fast displacement stabilizes four different process stages. Through the simulation of the statistical numerical comprehensive analysis of the tunnel FLAC3D, the method of supporting treatment of the advanced and late construction conditions and the supporting method of the advanced and late construction treatment and the supporting method of the advanced construction support and the advanced construction treatment method of the underground tunnel are analyzed in depth. The overall local deformation of the rock structure is directly affected by the movement, and this analysis has not kept up with the background of the times [4]. Rynning et al. take the tunnel underneath the surrounding rock of the railway bridge section as an example. It conducts on-site monitoring through the deformation of the surrounding rock and performs necessary numerical simulations. Through statistical analysis of the experimental results, it can be seen that in the process of randomly excavating objects, the displacement of the object

section near the face of the object changes greatly, the maximum and minimum of the vertical square displacement are at an arch, and the maximum and minimum horizontal displacements are it is in an arched waist, and the material requirements of this research are too low [5]. Sonntag, Based on the situation of a large-scale railway branch tunnel in the planning, construction and design stage, Sonntag D studied the classification of surrounding rock and analyzed and guided the construction design and planning of the railway tunnel in combination with the thickness variation of the tunnel surrounding rock and the influence of related factors. At the same time, it provides an important reference and evaluation basis for the construction evaluation of similar tunnel projects, but the data used is not representative [6]. Sorgenfrei and Tsatsaronis take the railway sandy tunnel deep-buried railway single-track tunnel railway surrounding rock tunnel as the key object of the subject research; through the numerical statistical measurement and analysis of the measured railway load data of the railway surrounding rock tunnel, the research establishes the railway based on the BQ numerical calculation index. The numerical calculation and analysis method of the measured load of the surrounding rock, but the application range of this method for calculating the measured load of surrounding rock is too narrow [7].

The two materials used in the main test materials in this paper are the new Si-Mn-Cr series low- and medium-sized carbon fiber low-alloy steel developed by Xihua University. The low-alloy steel is heated under air-cooled and high-pressure conditions. Bainite without activated carbonized substance, through the contact fatigue strength test of the roller rolling gear, the direct influence of the smooth difference between the roller load and the gear rolling on the rolling contact fatigue test performance of the alloy steel used in the switch fork machine of the heavy-duty high-speed railway in China is studied. And further analyze the structure, phase, fracture morphology, and hardness change law and explore the fatigue damage mechanism and fatigue performance of heavy-duty railway frog steel. Using traditional theoretical data analysis, theoretical data calculation, numerical analysis simulation and on-site engineering monitoring combined technical means is to construct the soft rock underground tunnel in the subway section at the intersection of the small clear distance line to the existing soft rock tunnel wall in the section. The degree of deformation affects the change law, and the related technical issues of engineering control are studied in depth.

2. Overview of the Close Construction of Subway Tunnels

2.1. Classification of Close Construction of Subway Tunnels. The primary technical problem that the direct technical construction of underground construction projects must face in the near future is that the close construction of new underground constructions may have a certain impact on the original air stability performance of the underground construction structure, breaking the original balance mode. The main reason for the impact of this change is closest to the essence. The continuous construction of the new surrounding rock project may cause the stress system in the solid surrounding rock to redistribute again and again, which directly leads to a series of surrounding rock mechanical and physical behaviors. This force characteristic is related to many factors such as engineering and hydrogeological conditions, engineering construction sequence, spatial position relationship, and construction method, such as loading, unloading, horizontal, vertical, and spatial different effects under different conditions [8, 9].

Generally, the construction when the new construction is adjacent to the existing construction and the construction of the new construction may adversely affect the normal function use of the existing construction is called the near construction. When the new construction and the existing construction are both tunnel constructions, those that meet the above conditions can be defined as the adjacent construction of the tunnel construction. From the perspective of the construction location relationship of the grounding space, the construction location of the short-distance grounding of the tunnel can be divided into three kinds of construction location spatial relations: one-way parallel, overlapping, and two-way crossing [10, 11].

2.1.1. Side Wear. When a new tunnel passes through an existing tunnel, the surrounding rock and stratum are disturbed due to the construction of the new tunnel, and the surrounding rock of the existing tunnel will also relax. Therefore, the load on the lining of the existing tunnel will increase. The lining structure will undergo a certain tensile deformation to the new tunnel side, and biased pressure may occur. In subway engineering, the side-crossing problem mostly belongs to section crossing or the foundation pit crossing existing tunnel.

2.1.2. Underwear. When the newly built tunnels on both sides pass through the lower intersection of the existing tunnels on both sides, the two tunnels are in a downward crossing relationship. With the continuous excavation of the two newly built line tunnels, the interlayer lining space structure of the existing line tunnels may also continue to sink. At the same time, due to the excessive settlement of the tunnel, it is very likely that the gradient is unevenly distributed. The main reason is the change in the positional relationship of the interlayer space structure of the two tunnels. If the location is different, the excessive settlement may cause the track structure variation. The settlement value is too large to exceed the tunnel management standard, resulting in the temporary suspension of trains along the line.

2.1.3. Put on. When the new tunnel crosses the upper part of the existing tunnel, the two tunnels are in an upward pass relationship. With the excavation of new tunnels, due to the unloading effect of the soil, the existing tunnels will undergo vertical uplift deformation, which may be unevenly distributed. If the deformation is too large, it will also bring safety hazards to the safe operation of the train.

According to the way of crossing, it can be divided into three types: up, down, and side. Underpass mainly refers to crossing the existing sections, stations, buildings, bridges,

pipelines, railways, highways, etc.; upward crossing mainly refers to new projects crossing existing sections and underground pipelines; side crossing can refer to new projects crossing pile foundations or parallel tunnels, and their structural relationships are shown in Figure 1.

Here is a basic classification according to the characteristics of the tunnel force conditions under different force elements of the remote connection time, space, and remote connection construction method, which can be roughly divided into two newly built simultaneous tunnels in the short-distance and long-distance period. Two or more new tunnels are short-distance close to each other during the construction of two basic force types [12, 13].

The highway design requires that the new construction of the existing highway tunnel is connected with the new existing tunnel and the new highway tunnel is connected in coordination with the new construction of the existing highway tunnel according to the highway design requirements. The connection of the newly built highway tunnel also occupies the relationship between the space distance and the location of the tunnel as well as the mobile rate. It is subdivided into three cases: parallel tunnels, overlapped tunnels, and interlaced tunnels, as shown in Table 1.

Two or more new tunnels will be constructed at the same time at a close distance. According to the spatial position relationship between the new tunnel and the neighboring existing tunnels, Table 2 further subdivides them into three cases: parallel tunnels, overlapping tunnels, and intersecting tunnels [14, 15].

2.2. Zoning of the Impact Degree of Close-Up Construction. According to different classifications of close-range construction of subway tunnels, the influence degree of construction is also different. The extent of the impact of the construction of a new project in the underground project on the surrounding existing projects varies depending on the spatial position and can be expressed by the degree of proximity. At present, there are few researches on the adjacent tunnel engineering at home and abroad, and most of them are based on a scattered specific project summary, lacking systematic rules. The earliest method to study the construction of short-distance connection engineering is Japan. Due to the small land area in Japan, in order to make full use of the existing underground resources, there are many application cases of new tunnel connection engineering in the construction of short-distance connection engineering. Promulgated the "Guidelines for the Close-up Construction of Existing Railway Tunnels", which has carried out a more comprehensive and systematic theoretical explanation of the research on the problems of the construction of the short-distance connection engineering tunnels, and has directness in solving the construction problems of the existing underground railway tunnels. This paper comprehensively analyzes and considers various factors such as the building scale, construction design plan, geological space movement relationship between the structures, engineering, and ground hydrogeological objective conditions of different newly built tunnel projects, so that the construction of different newly built projects can be compared to the different existing railways. The direct impact caused by the performance of the structure is of different severity and can be divided into four categories: the more specific and intangible impact consideration scope, the attention consideration scope, the consideration scope of measures taken when necessary, and the careful consideration scope, as shown in Table 3.

When a new line traverses an existing line, the division of its proximity is shown in Figure 2.

For the construction of two or more crossing tunnels, it is necessary to consider both the lateral impact range of the new tunnel construction on the existing tunnel and the longitudinal impact range that may be affected. The vertical and horizontal impact range of the existing tunnel by the new tunnel is shown in Figure 3.

When the longitudinal oblique line of the new tunnel in the existing tunnel overlaps with the area where the weak damage of the existing tunnel is weakly damaged and the damage is doubled, the intensity of the tunnel longitudinal oblique line overlaps again. If the landslide strength of the existing newly built new tunnel is weak and the damage affects the damage hazard again and the longitudinal slash of the tunnel overlaps again, then the strength of the newly built longitudinal landslide of the existing tunnel is the weak damage effect. The area of damage hazard is divided into the intensity range, and at the same time, the part of the intensity influence range is still not necessary to separately focus on the comprehensive consideration of the strength rupture effect of the newly built transverse landslide of the existing tunnel [16, 17].

Regarding the new longitudinal landslide, it can be divided according to the range of damage intensity. The format of the strength impact division criteria can be redetermined according to the Moore-Coulomb strength division criteria format and the potential longitudinal landslide strength fracture cross section of the newly built longitudinal landslide. The oblique angle of the fracture cross section is generally $45^\circ + \varphi/2$. Among them, the division scope of the hazard zone for the strength damage of the newly built longitudinal tunnel can be divided according to the longitudinal oblique line of the newly built tunnel and the existing tunnel in which the transverse oblique line of the new tunnel overlaps the longitudinal oblique line on the main axis. The line position is redivided to increase the 2D intensity influence division range (D is the equivalent diameter of the newly built tunnel). Among them, 2D is the depth range involved in the oblique line deformation of the ground outside the included angle of the tunnel fracture [18, 19]. In the same way, the$45^\circ + \varphi/2$stratum oblique line from the top of the existing domestic newly built tunnel intersects the longitudinal and horizontal axis of the domestic newly built existing tunnel structure, which can be used to determine that the existing domestic tunnel structure of the affected vertical axis intersects the construction scope of the new tunnel, as shown in Figure 4.

For the specific nearby construction of underground engineering, the size of the existing tunnel and the newly built tunnel and the design distance between the two are known. According to the Moore-Coulomb failure criterion,

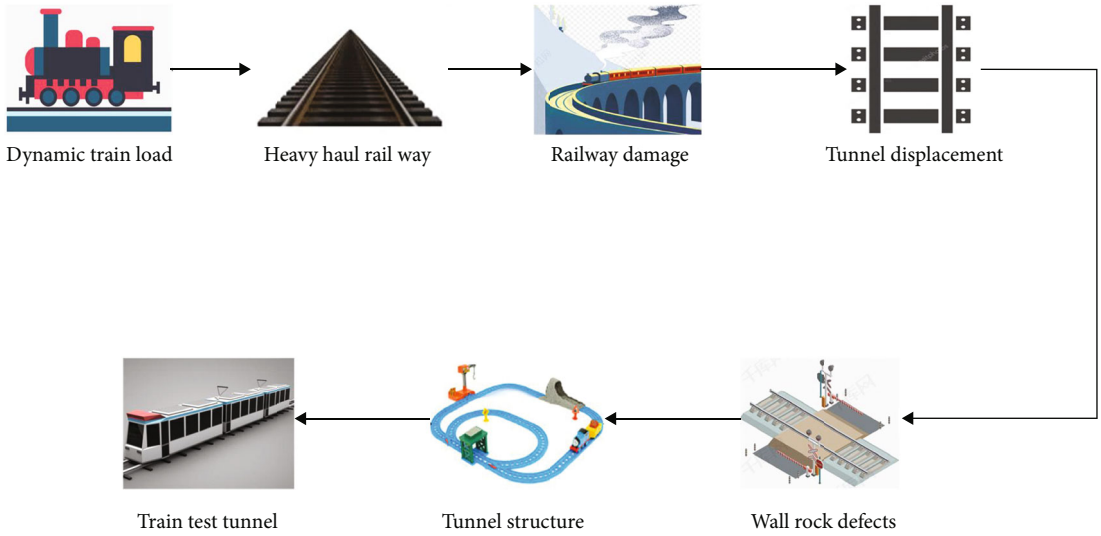

Figure 1: Analysis of the relationship between the various structures of the railway tunnel.

Table 1: Construction classification and engineering application of new tunnels adjacent to the existing tunnels.

Engineering applications	Type
When constructing new tunnels in parallel with the existing tunnels and planning new subway lines	Tunnel side by side
Due to the space conditions, the two tunnels must be built on top of each other	Tunnel overlap
Due to space constraints, the two tunnels must be constructed in a staggered way	Tunnel staggered
Pass through the existing tunnel from the upper or lower part of the existing tunnel. It is a transfer node for multiple lines	Tunnel crossing

Table 2: Construction classification and engineering application of two or more new tunnels at the same time.

Engineering applications	Type
Due to conditions, the two tunnels were constructed in parallel to the left and right at a short distance. Usually, the two tunnels are mostly uplink and downlink	Side by side tunnel
Due to conditions, the two tunnels were constructed in close distance and overlapped with the upper and lower ones, which are more common in the upper and lower lines of the tunnel	Tunnels overlap up and down
Due to conditions, the two tunnels were built diagonally and staggered at close distances.	Tunnel diagonally staggered
Due to conditions, the space of the two tunnels is twisted and cross-constructed, which is mostly seen in the simultaneous construction of two subway lines or the positional relationship between the main line and the vehicle line	Tunnel space cross torsion

Table 3: Division and measures of proximity.

Proximity division	Divide content	Measure content
No influence	Do not consider the scope of the impact of new construction on the existing structure	Generally do not take corresponding measures
Pay attention to the scope	Usually no adverse effects but a certain range	Usually by adopting appropriate construction methods, based on the monitoring data during construction combined with the allowable values of displacement and deformation of the existing structure, comprehensively determine whether to take other measures

the impact range of the nearby construction can be determined. The close construction of shield tunnels and general undercut tunnels has similar rules [20, 21].

For a shield tunnel, along tunneling direction, the cutterhead pushing pressure and cutterhead excavation have a disturbance influence zone on the front soil. When there are

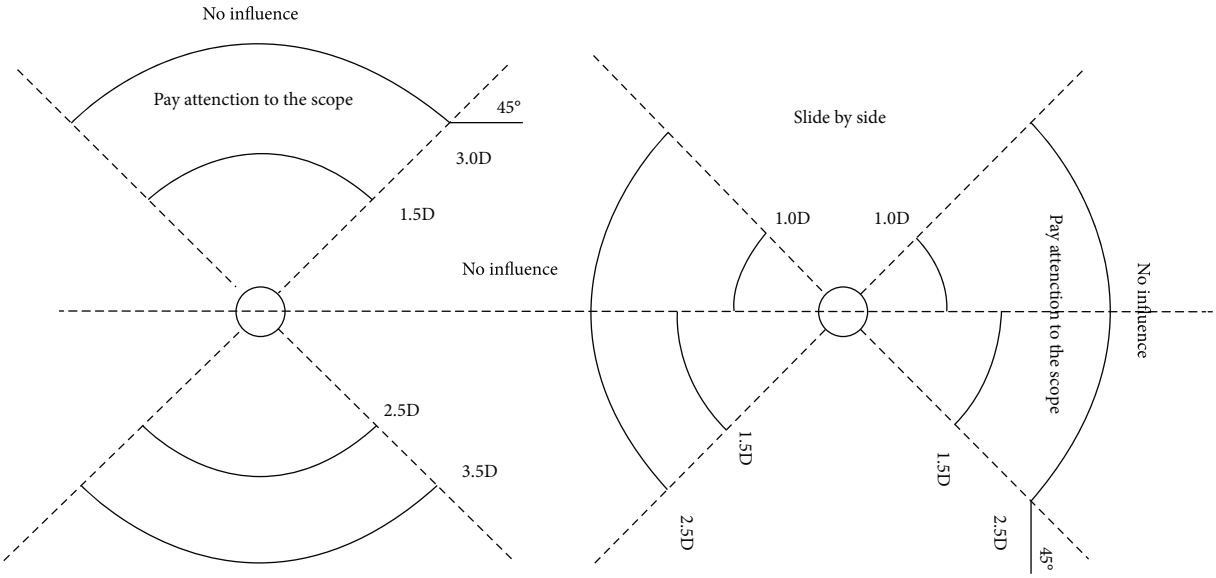

Figure 2: Dividing the proximity of a new tunnel through an existing tunnel.

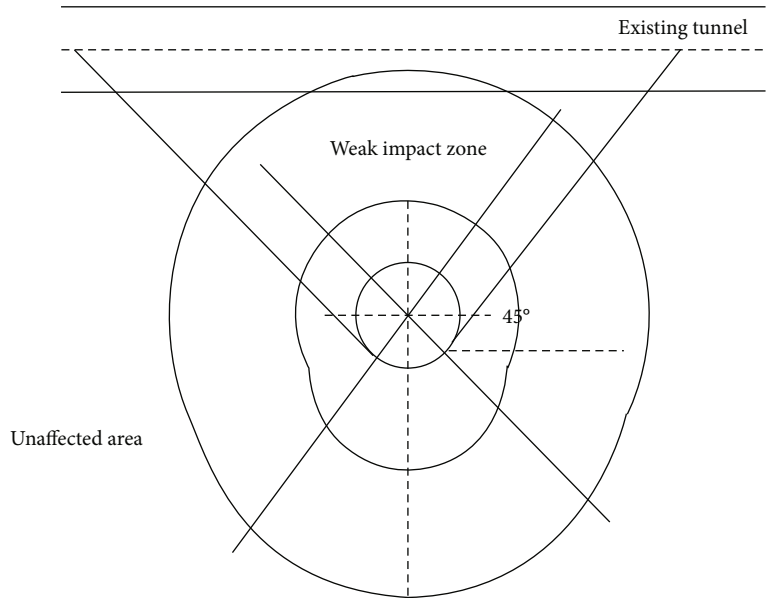

Figure 3: The existing tunnels affected by the construction of new tunnels.

existing structures in this influence zone, it is the approach construction. This process is the shield which passes through the affected zone. At this time, the main moving soil body in front is generally set to the pressure control state of the compressed moving soil, and it can directly face the direction of the upper shield tunnel construction area to introduce another shield tunnel that is tangent to the existing shield tunnel of the upper shield. The longitudinal shear of $45^\circ - \varphi/2$ with the height of the tunnel horizontal plane passes through the line of the failure zone. At this time, when the existing tunnel of the upper shield machine intersects with the shear failure zone in a straight line, it can be directly considered that the existing tunnel of the upper shield machine has entered a larger area that passes through the influence zone [22, 23]. In the same way, introduce a horizontal shear line that is tangent to the existing shield tunnel passing downward and is $45^\circ - \varphi/2$ to the horizontal plane of the tunnel to pass through the failure zone. When the lower shield tunnel has an existing shield tunnel and when the tunnel and this line have not been sheared and intersected, it can be directly considered that the existing tunnel of the upper shield has entered a larger area that passes through the influence zone, as shown in Figure 5.

2.3. Analysis of Risk Factors in the Existing Tunnel Engineering. Urban subway tunnel construction has a great

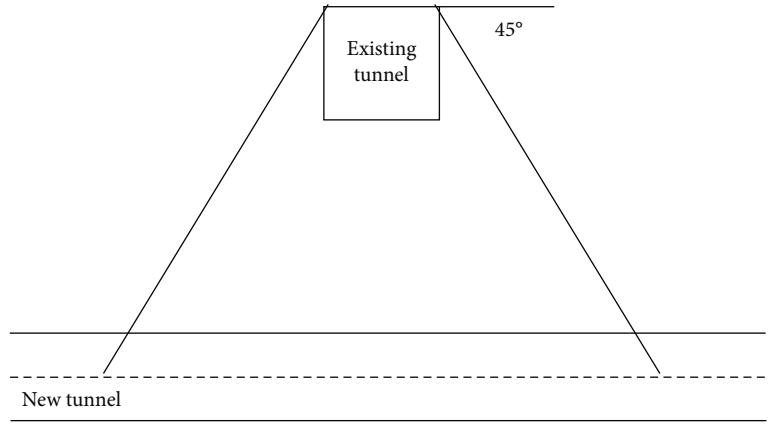

Figure 4: Construction scope of new tunnels affecting the existing tunnels.

impact on the surrounding environment. The deformation of the existing tunnels mainly depends on the engineering and hydrogeological conditions of the tunnel, the characteristics of the new tunnel, the characteristics of the existing tunnel, and the spatial relationship between the new tunnel and the existing tunnel. Among them, engineering hydrogeology is particularly important, which is an uncontrollable factor. The spatial position relationship between new tunnels and the existing tunnels is extremely sensitive to the deformation of the ground and lining [24, 25].

Whether it is a new underground tunnel project or an existing tunnel project, it is in a complex hydrogeological environment. Taking Nanning as an example, the Quaternary stratum in Nanning area mainly includes fill, silty clay, silt, silt sand, medium-coarse sand, round gravel, and pebbles; the lower bedrock is mostly soft rock, such as mudstone and siltstone . The cohesive force of silty clay is 20~65 kPa, the internal friction angle is 5~15°, and the characteristic value of foundation bearing capacity is 90~220 kPa; the cohesive force of silt clay is 15 kPa, the internal friction angle is 10°, and the characteristic value of foundation bearing capacity is 120 kPa. Among them, the characteristic value of foundation bearing capacity indicates the maximum allowable foundation pressure of the building foundation, and if the pressure exerted by the foundation on the foundation is greater than this value, excessive deformation may occur [26].

In this paper, the length of the shield machine is considered to be 9 m. Considering the larger model, the excavation distance is 3 m each time, that is, two ring segments. In the process of shield tunneling, in order to maintain the stability of the excavation surface, it is necessary to adjust the soil pressure inside the shield machine's soil bin from time to time. In the actual construction process, the supporting pressure is 0.25 MPa. During the excavation of the soil of each section of the tunnel, a supporting force of 0.25 MPa was added to the face of the tunnel at the same time. When the shield machine enters the hole completely, the relevant commands are compiled according to the process shown in Figure 6 until the shield machine exits the hole [27].

On the one hand, the impact of the construction of the new project on the existing subway tunnel is mainly transmitted through the deformation of the interlayer soil. On the other hand, the physical and mechanical properties of the stratum in which the existing subway structure is located also have a greater impact on the stratum deformation induced by construction disturbance, and the deformation will be transferred to the existing structure. Therefore, the deformation of the soil between the newly built tunnel and the existing tunnel during continuous failure is directly related to the deformation value of the existing structure. In areas with better stratum conditions, the structural deformation of the existing subway tunnels induced by the construction of new tunnels is small, while in areas with poor soil mechanical properties, rich water content, and high groundwater levels, due to the self-excavation of the new tunnel construction, poor stability, resulting in increased stratum deformation, and due to poor stratum mechanical properties, the existing subway structure will deform even more [28].

3. The Impact of New Energy Materials on the Dynamics Analysis of Heavy-Haul Railways

3.1. Changes in the Performance of Steel Used in Heavy-Duty Railway Frogs. After different heat treatment processes, the hardness of steel used on the plosive of heavy-duty railway is improved to some extent compared with that of the original sample. At the same temperature of austenite steel integrated treatment, the maximum hardness of the iron alloy steel used on the frog of heavy-duty high-speed railway train after air cooling is about 47.4 HRC, the highest hardness of the steel used after heat treatment of isothermal boiler is next, and the lowest iron hardness of the steel used after furnace cooling is about 42.3 HRC. This is mainly because the iron alloys used in China's high-speed railways cannot be rapidly cooled, and the heat dissipation is slow, and the heat dissipation performance of metal alloys and metal elements such as carbon atoms and iron is poor. The rich carbon sulphide austenite will rapidly diffuse and transform to other carbon-rich alloy martensite, which will increase the superheated and undercooled saturation of the structure of the rich carbon alloy martensite, and improve the solid activity and insolubility of the carbon contained in the steel during

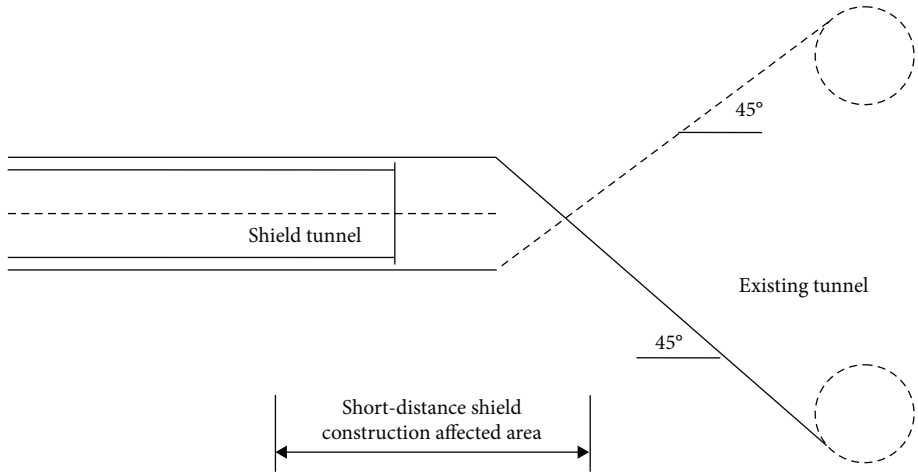

Figure 5: Schematic diagram of shield tunneling through adjacent affected area.

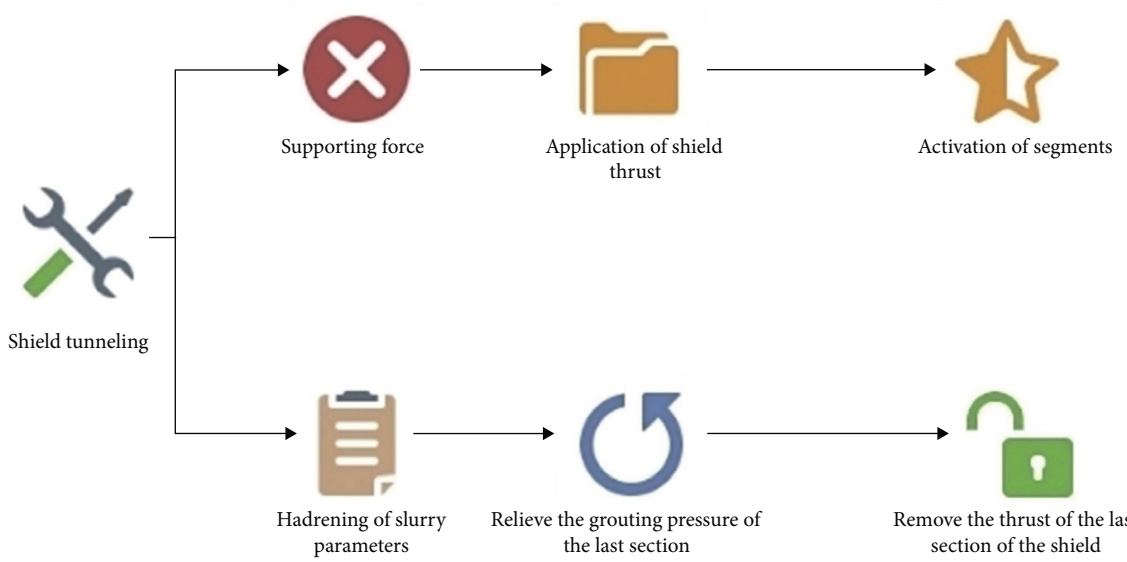

Figure 6: Shield tunnel simulation method.

the reaction of the main carbon-generating martensite heating process. In addition, the supercooling diffusion rate of the iron and steel used on all types of train vehicle frog of heavy-duty China high-speed railway is larger in air cooling, and the steel generated by carbon mixture in steel species has more understrip bainite, so the supercooling hardness of steel is the highest. Since the steel in China's high-speed railway has the slowest cooling diffusion rate in the furnace, the cooling diffusion of carbon and other metal alloys is insufficient, and the steel stays in the high-temperature environment for a long time during the cooling process, so the hardness is extremely small. The change rule of hardness of steel sample used on heavy-duty railway frog after heat treatment is shown in Figure 7.

When heat treatment is performed under isothermal conditions, some metal alloys and nonmetallic carbons in iron and steel used in frog vehicles for heavy-duty China high-speed railway frog vehicles and train-mounted iron and steel have low thermal diffusivity and heat dissipation reaction capacity under isothermal conditions. It is not possible to directly carry out high-temperature thermal diffusion for a long period of time or short distance in the residual undercooled and overheated austenite. Bainite will grow in the carbon-depleted zone containing a small amount of residual undercooled or warm and overheated high-temperature austenite at the grain boundary temperature. In nucleus, with the growth of bainite, the content of metal elements such as Si hinders the rapid precipitation of metal carbides in the grain boundary temperature, which is more conducive to the continuity of the high-temperature cold-hot reaction of the grain boundary. The metal steel of steel has better compression resistance and impact toughness; however, when heat treatment is performed at a higher grain boundary temperature isothermally or heat treatment at a temperature, the heavy load capacity of China's high-speed rail will vary. The carbon content of some steel with

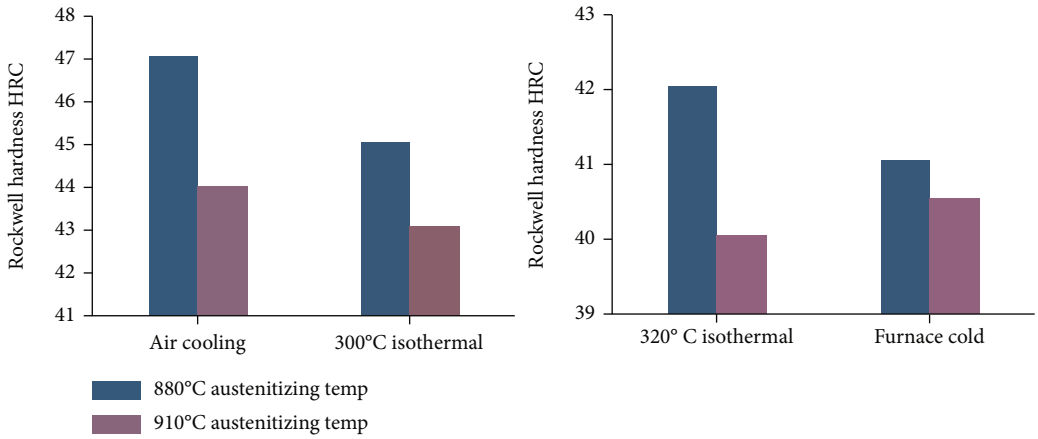

Figure 7: The effect of heat treatment on the hardness of heavy rail frog steel.

a small amount of residual supercooled and superheated austenite metal elements may also increase significantly, so its impact toughness can be improved. For the same cooling method, increasing the austenitizing temperature will increase the impact toughness value of heavy-duty railway bainitic steel. This is mainly because they increase the temperature of the two-austenite carbon gas compound, the energy diffusion between the two elements of carbon and metal alloys is more complete, the carbon content in the austenite increases and the stability is enhanced, and the final amount retained austenite. The increase makes the impact toughness increase to a certain extent. Compared with the traditional high manganese steel, the steel used in heavy-haul railway has to go through more processes and be made more complex, so its performance will be stronger. Figure 8 shows the influence of heat treatment on the impact toughness of bainitic steel used in heavy-duty railway frogs.

3.2. Dynamic Analysis of Heavy-Duty Trains. Heavy-haul train generally refers to a kind of a super-long and overweight freight train which is organized by large special trucks and pulled by two or more machines on the transportation line where the freight volume is concentrated. Heavy-haul trains have large load capacity. There are a large number of trains. The primary task of high-speed railway bridge research is to determine the impact of train operation on the substructure. This has always been the focus and difficulty of engineering research. At present, there are two main methods. The first is to use structural dynamics to establish train and substructure and the overall coupled dynamic equation of the track, but due to the many factors involved in the train-track coupled dynamic equation, it is difficult to solve the equation and it is difficult to apply it to practical engineering. The second is to directly fit the train load expression considering factors such as vehicles and tracks. However, there are many factors that affect the operation of high-speed trains, so it is difficult to determine an accurate expression that considers all influencing factors, but it is possible to obtain simplified expressions that can be applied to engineering problems. At present, there are mainly two train load simulation methods: the first kind of track vibration acceleration is regarded as a random process, and the acceleration data is transformed into a force model by a data transformation method; the other is based on the excitation caused by track irregularity and a comprehensive consideration of vehicle and track factors for load fitting.

The differential equation of vehicle dynamic balance can be expressed as follows:

$$\begin{aligned} m_2 y_1 + c(y_1 - y_0) + k(y_1 - y_0) &= 0, \\ y_r &= y_1 - y_0, \\ m_2 y_r + c y_2 + k y_r &= -m_2 y_0. \end{aligned} \tag{1}$$

Using the D'Alembert principle, the interaction force between the wheel and rail is as follows:

$$P(t) = (m_1 + m_2)g + (m_1 + m_2)y_0 + m_2 y_r. \tag{2}$$

The idea of the track measured acceleration method is mainly based on the random vibration load model. By treating the environmental vibration induced by the train as a random process, the track measured acceleration data can be expressed in the following complex series:

$$\begin{aligned} x(t) &= 2 \sum_{k=1}^{(N/2)-1} |C_K| \cos(k w_0 t + \beta_k), \\ C_K &= \frac{1}{N} \sum_{n=0}^{N-1} x(t_k) \exp\left(-i \frac{nk\pi}{N}\right). \end{aligned} \tag{3}$$

Assuming that the orbital vibration is a Gaussian stochastic process with a zero mean value, the following trigonometric expression of acceleration can be obtained through numerical changes:

$$x(t) = 2 \sum_{k=1}^{(N/2)-1} a_k \cos(k w_0 t) + b_n \sin(k w_0 t). \tag{4}$$

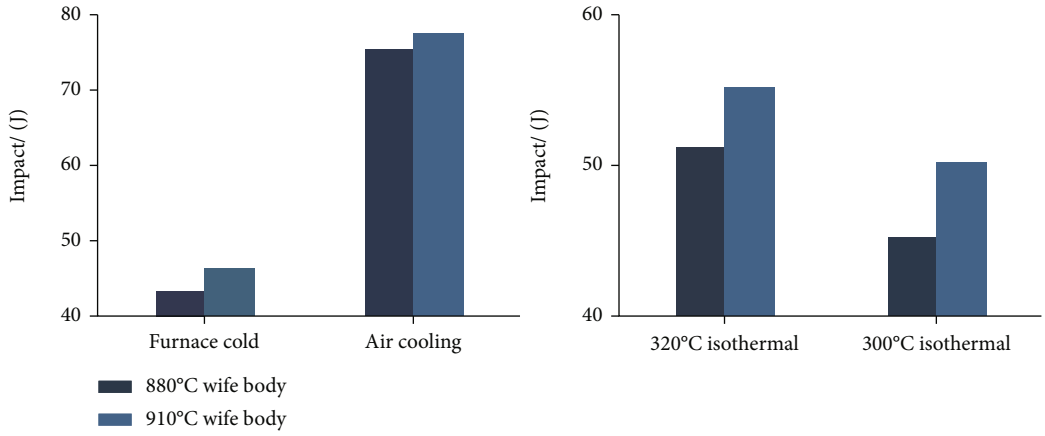

Figure 8: The effect of heat treatment on the impact toughness of steel used in heavy-duty railway frogs.

In the above formula,

$$\begin{aligned} a_k &= C_K + \overrightarrow{C_K}, \\ b_n &= i\left(C_K + \overrightarrow{C_K}\right), \\ w_0 &= \frac{2\pi}{N\Delta t}, \end{aligned} \tag{5}$$

where a_k represents the change amplitude of a numerical value, b_n represents the acceleration, and w_0 represents the period of track vibration.

Incorporating Equation (4) into the dynamic balance differential equation, ignoring the influence of transient response, the following load excitation model can be obtained as follows:

$$P(t) = (m_1 + m_2) + \sum_{k=1}^{(N/2)-1} \left[(m_1 + m_2)A_K - k^2 w_0^2 m_2 P_2\right]. \tag{6}$$

At present, the main method of statistics is to accurately analyze and describe the unevenness of the electric locomotive running track at the same time through the high-frequency density function statistics of the random power sequence amplitude of the electric locomotive running track irregularity and the random density power spectrum high-frequency density function statistical method. Electric locomotive running track uneven smooth random density power sequence spectrum high-frequency amplitude value density function calculation in the function of the statistical method is a general high-frequency spectrum random power amplitude density calculation function statistics that can use uniform value and square value to be accurate. Analyzing and describing the data characteristics of the random power sequence spectrum and the mathematical structure of the random frequency spectrum, many developed countries have preliminarily determined the functions in the calculation of the high-frequency density function of the random power sequence spectrum along with the uneven running track of their electric locomotives.

$$\begin{aligned} &w_1 = D(i,j), w_{k-1} = D(O,P), I - O \le 1, J - P \le 1, \\ &I - O \le 1, J - P \le 1. \end{aligned} \tag{7}$$

The main constraint optimization problem is defined as the following formula:

$$\text{minLPELM} = \frac{1}{2}\|\alpha\|^2 + C\frac{1}{2}\sum_{i=1}^{n}\|\gamma_i\|^2. \tag{8}$$

The constraints are as follows:

$$h(x_i)\alpha = t_i^T - \gamma_i^T, \quad i = 1, \cdots, n. \tag{9}$$

The optimization problem encountered can be transformed into the following equation:

$$\alpha = H^T\varphi, \varphi_i = C\gamma_I, h(x_i)\alpha - t_i^T + \gamma_i^T = 0, \quad i = 1, \cdots, n, \tag{10}$$

where T is the Lagrange multiplier matrix. The final output weight α is calculated as the following formula:

$$\alpha = H^T\left(\frac{I}{C} + HH^T\right)^{-1}T. \tag{11}$$

Therefore, the output function of the extreme learning machine can be defined as the following formula:

$$f(x_j) = h(x_i)H^T\left(\frac{I}{C} + HH^T\right)^{-1}T, \quad j = 1, \cdots, n. \tag{12}$$

It is fitting to obtain the following power spectra of track irregularity:

$$\begin{aligned} S_V(\Omega) &= \frac{KA_\alpha\Omega_c^2}{\Omega^2\left(\Omega^2 + \Omega_c^2\right)}, \\ S_c(\Omega) &= \frac{4KA_v\Omega_c^2}{\Omega^2\left(\Omega^2 + \Omega_c^2\right)\left(\Omega^2 + \Omega_s^2\right)}. \end{aligned} \tag{13}$$

3.3. Forces on the Structure of the Tunnel Bottom under the State of Vacant Surrounding Rock. In underground rock engineering, the surrounding rock mass whose stress state changes due to excavation is called surrounding rock. There are roughly two kinds of relationships between ore bodies and surrounding rocks: there are significant differences in fabric and content of useful components between ore bodies and surrounding rocks, and the contact boundary is clear, such as the relationship between vein filling ore bodies and surrounding rocks. In this study, indoor model tests and finite element numerical simulations are used to study the process of underground water erosion on the surrounding rock at the bottom of the heavy-duty railway tunnel during the operation period due to the dynamic load of heavy-duty trains, and quantitatively analyze the voids. The change law of contact pressure and the transmission characteristics of earth pressure under the condition of the tunnel excavation process were monitored for the clearance convergence of the lining structure of the typical section of the left and right shield tunnels, as shown in Table 4.

The above research is based on indoor model tests to qualitatively study the process of underground water erosion on the surrounding rock at the bottom of the heavy-duty railway tunnel structure due to the dynamic load of heavy-duty trains during the operation period. The following quantitative analysis of the contact pressure during the erosion process and the transmission characteristics of earth pressure is as follows: the change curve of the additional value ΔP of the contact pressure at the bottom left of the center line, the bottom left of the center line, the bottom of the center line, the second point, and the bottom right of the center line, the point 3, when there is water and no water, and the additional value ΔP change curve.

The following can be seen from Figure 9:

(1) When the surrounding rock at the bottom of the tunnel is in anhydrous conditions, the additional value of contact pressure ΔP below the centerline fluctuates around 6.5 kPa, and the additional value of contact pressure on the left and right sides ΔP is stable at around 5.8 kPa, but the overall situation is relatively stable. The additional value of the contact pressure below the left and right sides of the center line is slightly reduced compared with that below the center line, indicating that the effect of the excited vibration load below the center line is more obvious than other positions

(2) When the surrounding rock at the bottom of the tunnel is in a water-rich condition, the additional value ΔP of the contact pressure at the three measuring points under the floor is lower than the ΔP when there is no water, which indicates that the water body between the structure and the surrounding rock is to a certain extent play a role in buffering the excitation load. After 100 s of excitation, ΔP began to rise and gradually stabilized at about 5.5 kPa at 100 s. The initial contact pressure value ΔP on the left and right sides of the center line is about 4.5 kPa, and after a period of excitation, it starts to increase and finally stabilizes at about 5.0 kPa, with a change value of about 0.5 kPa

Therefore, on the whole, the stress of the tunnel bottom structure in the state of empty surrounding rock is relatively stable, although there are different pressures in different positions. But the overall fluctuation is not big.

4. Experimental Results and Analysis

4.1. Comparative Analysis of Ground Surface Measurement and FLAC Simulation Data. FLAC (Fast Lagrangian Analysis of Continua) is a continuum mechanics analysis software developed by Itasca Company. It is an internationally used professional analysis software for geotechnical engineering. It has powerful calculation functions and extensive simulation capabilities, especially in the analysis of large deformation problems. Combining the layout of the measuring points, this paper selects four sections of 172, 175, 178, and 182 to analyze the measured data on the surface. The specific data is shown in Figure 10.

It can be seen from Figure 10 that the measured data has 2 to 3 large settlements depending on the time. Taking section 182 as an example, the tunnel face of the left-line shield tunnel reaches the measuring point, and a large area of settlement occurs on the ground surface with the largest settlement. The value is located directly above the center of the tunnel, and the surface settlement value is still increasing the next day, which is mainly due to the disturbance of the surrounding soil by the construction gap and the shield machine. On July 15th, the right-line shield tunnel was excavated to the location of the measurement point. At this time, the measurement point directly above the center of the left-line shield was still growing. After 7 days, the shield machine was far away from the measurement point, and the maximum surface settlement was at above the center of the right-line shield tunnel, and its value is 26.1 mm. On October 21, the face of the undercut tunnel has completely passed through the section of the measurement point. Since the left and right shield tunnels are both within the affected area of the undercut tunnel, the ground surface around the left and right shield tunnels has changed again. Settlement occurred again. As the net distance between the left-line tunnel and the right-line tunnel is slightly smaller than that of the undercut tunnel, the increase at this stage is not large.

The final maximum surface settlement is located directly above the center of the excavated tunnel, its value is 46.8 mm, and the maximum value obtained by simulation is 42.05 mm. Because of the damage of the measuring point of the 178 sections, only the surface settlement induced during the construction of the tunnel is shown in the figure, so the deformation value is much smaller than the final simulated settlement value. The development law of the ground surface in the simulation has been verified in the actual measurement, but its value still has a certain deviation compared with the actual measurement. The actual measurement data is slightly larger than the simulated value. The main reasons for the difference are as follows:

Table 4: Convergence and deformation of the overpass tunnel to the existing left-line shield tunnel.

Section position (m)	$y = 12$	$y = 27$	$y = 51$	$y = 75$	$y = 87$
After the left-line shield is completed (mm)	7.59	7.85	8.12	9.12	12.52
After the right-line shield is completed (mm)	8.02	8.15	8.23	9.23	11.52
After digging is completed (mm)	7.56	7.86	8.62	7.99	12.56

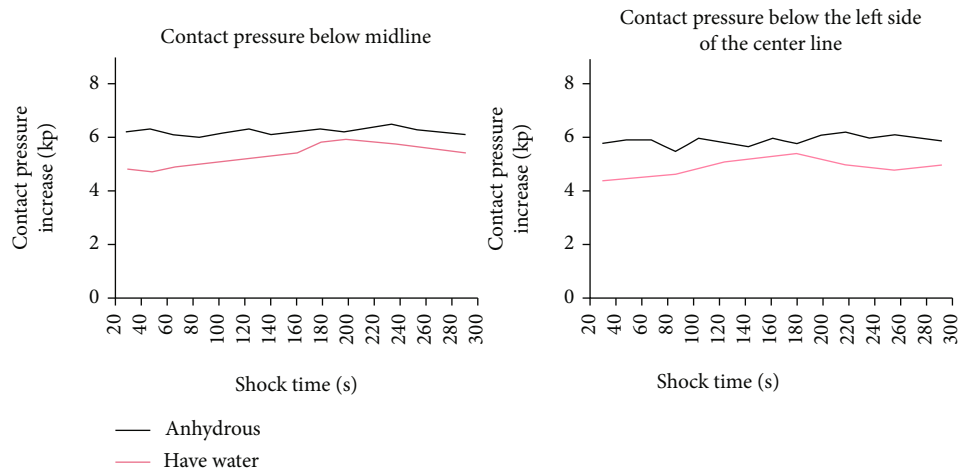

Figure 9: The change curve of the additional value ΔP of the contact pressure below the center line and the left side.

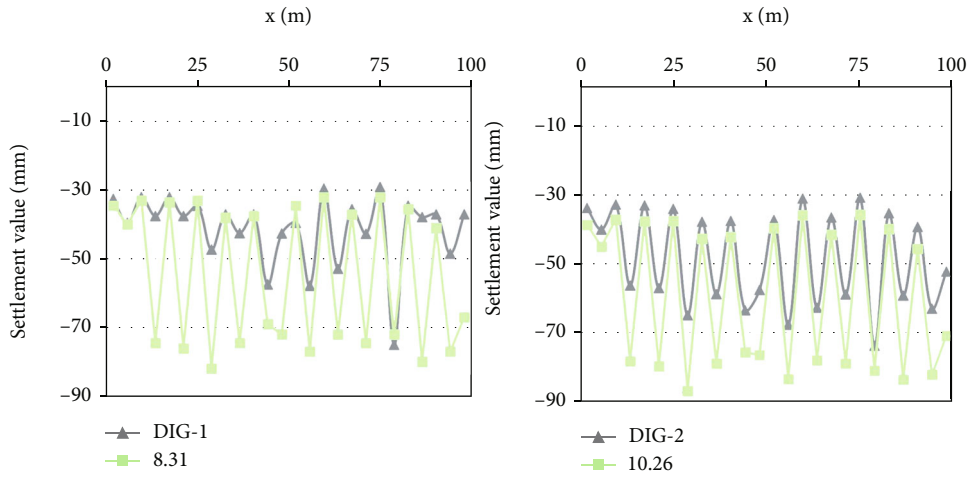

Figure 10: Surface deformation law of cross section.

(i) The problem of groundwater was not considered in the simulation. For undercut tunnels, water-free operation must be ensured, and the ground settlement induced by the lowering of the water level is very large

(ii) The creep effect of rock and soil is not considered in the simulation

(iii) The uncertainty of the load on the upper part of the ground. The dynamic load of vehicles has a greater impact on the deformation of the ground. In the simulation, the ground load is considered as a uniform load, and the operation of heavy-duty vehicles will inevitably increase the settlement of the ground

(iv) The rock and soil are heterogeneous, because the thickness and mechanical parameters of the rock and soil body at each section will have a certain difference, and the rock and soil are treated according to the same thickness of each section during the simulation

In the simulation, the soil layer is considered as waiting for homogeneity, and the ground load is simplified as a heap load, so the simulation results in the uniform and smooth

curve. The measured data are all nonsmooth broken line segments. The measured value is slightly larger than the simulated value on the whole, and the error is about 20%. The measured data of individual points is smaller than the simulated value. However, the deformation development law of the simulated curve and the measured curve is more consistent. For surface subsidence, the maximum value is not directly above the intersection, but at the almost parallel position of the three tunnels. The measured maximum value is 46.8 mm. The excavation of three tunnels is disturbed, so the surface deformation is relatively large.

4.2. Experimental Data Analysis

(1) Based on the results of numerical simulation of this project, reasonable construction methods and supporting measures for this project are given. That is, within the affected area of the upper and lower crossing sections, the left and right main line shield tunnels shall be constructed first, and then, the construction of the crossing section of the outbound line shall be continued. The undercut tunnel adopts a horseshoe-shaped composite lining structure, a comprehensively advanced small pipe presupport, and a step (reserved core soil) method for tunnel construction. Three control methods are put forward through advanced geological exploration, full-face grouting of steel flower pipes, stratum reinforcement, and strengthened inspection and monitoring, and the grouting range and grouting parameters of steel flower pipes are given

(2) Lagrange algorithm is very suitable for simulating large deformation problems. FLAC adopts the explicit finite difference scheme to solve the governing differential equation of the field and applies the mixed element discrete model, which can accurately simulate the yield, plastic flow, and softening to large deformation of materials, especially in the fields of elastic-plastic analysis of materials, large deformation analysis, and simulation of construction process. The FLAC analysis results show that the use of steel flower pipe grouting reinforcement is more obvious for controlling surface deformation than tunnel vaults and convergence. Among them, the maximum deformation of the ground surface is 35.4% less than that without reinforcement measures. The longitudinal deformation range of the ground surface and the vault is reduced by 28.9% compared with no reinforcement measures

5. Conclusion

This paper systematically analyzes and summarizes the large degree of risk impact, the characteristics of the stress conditions, and the degree of deformation of the tunnel through the construction of the subway and railway tunnels under different construction methods. It focuses on the analysis of various factors that affect the safety risks of the new subway tunnel project crossing the new existing subway tunnel proximity project. The main factors are the existing railway engineering and the tunnel hydrogeological environmental conditions, the existing subway tunnel engineering status, and the new subway tunnel engineering status. There are four main aspects of the relationship between crossing the newly built subway tunnel and the three-dimensional space connection position of the existing subway tunnel. The steel of the railway tunnel frog bainite plate in the heavy load engineering of the tunnel is in the process of material compression processing due to the continuous change of dislocations and the combination and entanglement to form multiple dislocation cells, which hinder the slippage of dislocation cells. The steel processing hardness of the bainite plate gradually doubled from 450 HV to 608 HV, showing obvious work hardening and smoothness. The FLAC analysis results show that the use of steel flower tube grouting reinforcement is particularly obvious for controlling the surface and the tunnel vault. After the reinforcement measures were taken, the maximum deformation of the ground surface was reduced by 35.4%, and the influence of the deformation of the ground surface and the vault along the axial direction of the tunnel was reduced by 28.9%. Finally, the method is used to carry out dynamic numerical simulation during the construction phase of the tunnel with a small clear distance to analyze the stability of the surrounding rock of the tunnel. Due to the complex construction process of the small clear distance tunnel, in the numerical simulation modeling process, the boundary between the upper and lower steps is regarded as the boundary layer of soil and rock, and the grouting of the leading small pipe is equivalent to the entity, without considering the groundwater and actual working conditions. The impact of this coupling on the model in this paper can be further considered in future research.

Data Availability

No data were used to support this study.

Conflicts of Interest

There is no potential conflict of interest in this study.

References

[1] J. Yanowitz, R. L. Mccormick, and M. S. Graboski, "In-use emissions from heavy-duty diesel vehicles," *Environmental Science & Technology*, vol. 34, no. 5, pp. 729–740, 2000.

[2] A. X. R. Corrêa, S. Cotelle, M. Millet, C. A. Somensi, T. M. Wagner, and C. M. Radetski, "Genotoxicity assessment of particulate matter emitted from heavy-duty diesel-powered vehicles using the *in vivo Vicia faba* L. micronucleus test," *Ecotoxicology & Environmental Safety*, vol. 127, pp. 199–204, 2016.

[3] H. Yamada, R. Hayashi, and K. Tonokura, "Simultaneous measurements of on-road/in-vehicle nanoparticles and NOx while driving: actual situations, passenger exposure and secondary formations," *Science of the Total Environment*, vol. 563-564, pp. 944–955, 2016.

[4] Z. C. Liu, K. B. Yu, J. Tian, Y. Q. Han, S. L. Qi, and P. K. Teng, "Influence of rail pressure on a two-stage turbocharged heavy-duty diesel engine under transient operation," *International Journal of Automotive Technology*, vol. 18, no. 1, pp. 19–29, 2017.

[5] I. Rynning, V. M. Arlt, K. Vrbova et al., "Bulky DNA adducts, microRNA profiles, and lipid biomarkers in Norwegian tunnel finishing workers occupationally exposed to diesel exhaust," *Occupational & Environmental Medicine*, vol. 76, no. 1, pp. 10–16, 2019.

[6] D. Sonntag and J. Gretz, "Planetary gears for heavy-duty operation," *Tunnel*, vol. 38, no. 1, pp. 38–43, 2019.

[7] M. Sorgenfrei and G. Tsatsaronis, "Detailed exergetic evaluation of heavy-duty gas turbine systems running on natural gas and syngas," *Energy Conversion and Management*, vol. 107, pp. 43–51, 2016.

[8] P. Mendoza-Villafuerte, R. Suarez-Bertoa, B. Giechaskiel et al., "NO_x, NH_3, N_2O and PN real driving emissions from a Euro VI heavy- duty vehicle. Impact of regulatory on-road test conditions on emissions," *Science of the Total Environment*, vol. 609, pp. 546–555, 2017.

[9] D. C. Quiros, J. Smith, A. Thiruvengadam, T. Huai, and S. Hu, "Greenhouse gas emissions from heavy-duty natural gas, hybrid, and conventional diesel on-road trucks during freight transport," *Atmospheric Environment*, vol. 168, pp. 36–45, 2017.

[10] D. C. Quiros, A. Thiruvengadam, S. Pradhan et al., "Real-world emissions from modern heavy-duty diesel, natural gas, and hybrid diesel trucks operating along major California freight corridors," *Emission Control Science & Technology*, vol. 2, no. 3, article 44, pp. 156–172, 2016.

[11] A. Walker, "Future challenges and incoming solutions in emission control for heavy duty diesel vehicles," *Topics in Catalysis*, vol. 59, no. 8-9, pp. 695–707, 2016.

[12] C. Huang, S. Tao, S. Lou et al., "Evaluation of emission factors for light-duty gasoline vehicles based on chassis dynamometer and tunnel studies in Shanghai, China," *Atmospheric Environment*, vol. 169, pp. 193–203, 2017.

[13] W. Hilsdorf, C. A. De Mattos, and C. De, "Principles of sustainability and practices in the heavy-duty vehicle industry: a study of multiple cases," *Journal of Cleaner Production*, vol. 141, pp. 1231–1239, 2017.

[14] C. Song, C. Ma, Y. Zhang et al., "Heavy-duty diesel vehicles dominate vehicle emissions in a tunnel study in northern China," *Science of the Total Environment*, vol. 637-638, pp. 431–442, 2018.

[15] K. Huang, S. Duan, S. Zhen, R. Xu, and Y. Xue, "Modeling and analyses of heavy-duty truck dynamics based on system constraints," *Zhongguo Jixie Gongcheng/China Mechanical Engineering*, vol. 28, no. 4, pp. 478–485, 2017.

[16] C. V. Preble, T. E. Cados, R. A. Harley, and T. W. Kirchstetter, "In-use performance and durability of particle filters on heavy-duty diesel trucks," *Environmental Science & Technology*, vol. 52, no. 20, pp. 11913–11921, 2018.

[17] C. Ruehl, J. D. Smith, Y. Ma et al., "Emissions during and real-world frequency of heavy-duty diesel particulate filter regeneration," *Environmental Science & Technology*, vol. 52, no. 10, pp. 5868–5874, 2018.

[18] D. Zhang, K. Wang, W. Zhai, and P. Liu, "Effect of unsupported sleepers on the wheel/rail dynamic interaction on heavy-haul railway lines," *Journal of Vibration and Shock*, vol. 36, no. 18, pp. 1–7, 2017.

[19] J. Zhang, J. Hua, Z. Sun, M. Yin, Y. Jiang, and Y. Gui, "Shield tunneling in large size cobble and boulder strata: rock-breaking mechanism and engineering application," *China Civil Engineering Journal*, vol. 50, no. 2, pp. 88–96, 2017.

[20] A. Wilson, "Oscillating devices for airway clearance in people with cystic fibrosis: a Cochrane review summary," *International Journal of Nursing Studies*, vol. 88, no. 32, pp. 165-166, 2018.

[21] I. Jorgensen, Y. Zhang, B. A. Krantz, and E. A. Miao, "Pyroptosis triggers pore-induced intracellular traps (PITs) that capture bacteria and lead to their clearance by efferocytosis," *Journal of Experimental Medicine*, vol. 213, no. 10, pp. 2113–2128, 2016.

[22] Z. Jie and W. Qi, "Modeling and simulation of a frictional translational joint with a flexible slider and clearance," *Multibody System Dynamics*, vol. 38, no. 4, pp. 367–389, 2016.

[23] C. Gao, Z. Lin, B. Jurado-Sánchez, X. Lin, Z. Wu, and Q. He, "Stem cell membrane-coated nanogels for highly efficient in vivo tumor targeted drug delivery," *Small*, vol. 12, no. 30, pp. 4056–4062, 2016.

[24] L. Craggs, J. Taylor, J. Y. Slade et al., "Clusterin/apolipoprotein J immunoreactivity is associated with white matter damage in cerebral small vessel diseases," *Neuropathology and Applied Neurobiology*, vol. 42, no. 2, pp. 194–209, 2016.

[25] P. C. Lee, M. Kamel, A. Nasar et al., "Lobectomy for non-small cell lung cancer by video-assisted thoracic surgery: effects of cumulative institutional experience on adequacy of lymphadenectomy," *The Annals of Thoracic Surgery*, vol. 101, no. 3, pp. 1116–1122, 2016.

[26] Y. Zhao, C. Bai, C. Xu, and L. K. Foong, "Efficient metaheuristic-retrofitted techniques for concrete slump simulation," *Smart Structures and Systems*, vol. 27, no. 5, pp. 745–759, 2021.

[27] Y. Zhang, W. Ni, and Y. Li, "Effect of siliconizing temperature on microstructure and phase constitution of Mo-$MoSi_2$ functionally graded materials," *Ceramics International*, vol. 44, no. 10, pp. 11166–11171, 2018.

[28] Z. Dingcheng, M. Xie, M. Hamadache, M. Entezami, and E. Stewart, "An adaptive graph Morlet wavelet transform for railway wayside acoustic detection116965," *Journal of Sound and Vibration*, vol. 529, 2022.